Tikrit Journal of Engineering Sciences (2024); 31(1): 182-192
DOI: http://doi.org/10.25130/tjes.31.1.16

IRAQI Academic Scientific Journals

ISSN: 1813-162X (Print); 2312-7589 (Online)
Tikrit Journal of Engineering Sciences
available online at: http://www.tj-es.com

TJES Tikrit Journal of Engineering Sciences

Adsorption of Congo Red Dye from Aqueous Solutions Using an Eco-Friendly Adsorbent Derived from Buckthorn Fruits

Ahmed K. Ibrahim [a*], Salwa H. Ahmed [a], Riedh A. Abduljabbar [b]
a Department of Environmental Engineering, College of Engineering, Tikrit University, Tikrit, Iraq.
b Department of Biology, College of Science, Tikrit University, Tikrit, Iraq.

Keywords:
Adsorption; Aqueous Solutions; Biochar; Buckthorn Fruit; Congo Red.

Highlights:
- It is possible to produce activated carbon from available, cheap and Eco-friendly agricultural materials.
- Adsorption is a surface phenomenon that can be used to remove some pollutants.
- Water contamination with dyes, including Congo red dye, comes from the textile or medical industry.

ARTICLE INFO
Article history:

Received	28 Dec.	2022
Received in revised form	17 Apr.	2023
Accepted	14 Dec.	2023
Final Proofreading	23 Jan.	2024
Available online	03 Mar.	2024

© THIS IS AN OPEN ACCESS ARTICLE UNDER THE CC BY LICENSE. http://creativecommons.org/licenses/by/4.0/

Citation: Ibrahim AK, Ahmed SH, Abduljabbar RA. **Adsorption of Congo Red Dye from Aqueous Solutions Using an Eco-Friendly Adsorbent Derived from Buckthorn Fruits**. *Tikrit Journal of Engineering Sciences* 2024; **31**(1): 182-192.
http://doi.org/10.25130/tjes.31.1.16

*Corresponding author:
Ahmed K. Ibrahim
Department of Environmental Engineering, College of Engineering, Tikrit University, Tikrit, Iraq.

Abstract: Dyes are used in the textile, paper, plastics, leather, foodstuff, and artificial fiber industries. Congo red dye (CR) is one of the dyes found in industrial wastewater. The present study investigates the Congo red dye removal from aqueous solutions using low-cost adsorbents that are eco-friendly and highly efficient, such as activated carbon prepared from Buckthorn fruit (BT) under various experimental conditions, as an ideal alternative to the current expensive methods for removing dyes from aqueous solutions. X-ray diffraction (XRD), Brunauer-Emmett-Teller (BET), scanning electron microscope (SEM), and Fourier-transformed infrared (FTIR) analyses were used for the fabricated-activated carbon characterization. Based on batch system experiments, various variables affecting the adsorption process were studied, including the solution's pH, adsorbent dose, contact time, initial dye concentration, and mixing speed. The results showed that the highest dye removal efficiency was 63% at pH = 5, the contact time was 80 minutes, the dose of adsorbent was 3 g/l, and the mixing speed was 150 rpm. The data from the experiments were analyzed using the Langmuir and Freundlich model and showed a high agreement with the Langmuir model (R^2 = 0.989). When studying the adsorption kinetics, the results agreed with the Pseudo-second order, where the values of K_2 and R^2 were 0.083g/mg. min and 0.992, respectively. The adsorption was endothermic and spontaneous, as shown by the thermodynamic parameters study at 25, 35, and 45 °C, where the ΔH was 13.709 kJ/mol and ΔG values were negative values. The study also showed the possibility of using Buckthorn fruit as a low-cost adsorbent in CR removal.

امتزاز صبغة الكونغو الحمراء من المحاليل المائية باستخدام مادة مازة صديقة للبيئة مشتقة من ثمار النبق

احمد خليل إبراهيم [1]، سلوى هادي احمد [1]، رياض عباس عبدالجبار [2]

[1] قسم هندسة البيئة / كلية الهندسة / جامعة تكريت / تكريت – العراق.

[2] قسم علوم الحياة / كلية العلوم / جامعة تكريت / تكريت – العراق.

الخلاصة

تستخدم الأصباغ على نطاق واسع لتلوين العناصر في صناعات النسيج والورق والبلاستيك والجلود والمواد الغذائية ومستحضرات التجميل والألياف الطبيعية والصناعية. صبغة الكونغو الأحمر (CR) صبغة مهمة توجد في مياه الصرف الصناعي. تهدف الدراسة الحالية إلى إزالة صبغة الكونغو الحمراء من المحاليل المائية باستخدام مواد ماصة منخفضة التكلفة وصديقة للبيئة وذات كفاءة عالية، مثل فاكهة النبق، في ظل ظروف تجريبية مختلفة، كبديل مثالي للطرق الحالية باهظة الثمن لإزالة الأصباغ من المحاليل المائية. تم توصيف الكاربون المنشط المحضر باستخدام تحاليل BET ,FTIR ,SEM و XRD. بناء على تجارب نظام الدُفعات، تمت دراسة المتغيرات المختلفة التي تؤثر على عملية الامتزاز، بما في ذلك الرقم الهيدروجيني للمحلول، وجرعة الممتزات، ووقت التلامس، وتركيز الصبغة الأولي، وسرعة الخلط. أظهرت النتائج أن أعلى كفاءة لإزالة الصبغة كانت 63% عند الأس الهيدروجيني = 5، وزمن التلامس 80 دقيقة، وجرعة المادة الماصة 3 غم / لتر، وسرعة الخلط 150 دورة في الدقيقة. تم تحليل البيانات من التجارب باستخدام نموذج Langmuir وFreundlich، وأظهرت توافقًا كبيرًا مع نموذج Langmuir (R^2 = 0.989). عند دراسة حركية الامتزاز أظهرت النتائج توافقًا مع الدرجة الثانية الزائفة حيث كانت قيمة K_2 و R^2 0.083 غم / ملغم / دقيقة و 0.992على التوالي. كان الامتزاز ماصًا للحرارة وتلقائيًا، كما يتضح من دراسة المعلمات الديناميكية الحرارية عند 25 و 35 و 45 درجة مئوية، حيث كانت ΔH 13.709 كيلوجول / مول وقيم ΔG كانت قيمًا سالبة. كما أوضحت الدراسة إمكانية استخدام ثمار النبق بكفاءة عالية كمادة ماصة ومنخفضة التكلفة في إزالة صبغة CR.

الكلمات الدالة: النبق، الامتزاز، الفحم الحيوي، الكونغو الاحمر، محاليل مائية.

1.INTRODUCTION

Water pollution with dyes is one of the widespread environmental problems [1]. Because of seeping from the soil, these contaminants also harm groundwater [2]. Dyes are the most common constituents of textile effluent. Some dyes have been linked to allergic dermatitis, skin irritation, cancer, and human mutation [3,4]. These dyes and their precursors are poisonous and carcinogenic, posing an environmental risk. Furthermore, their degradation frequently results in creating extremely carcinogenic aromatic amines. Hence, thorough treatment for polluted water is required when recycling wastewater [5]. One major dye discovered in wastewater is Congo red dye (CR), which has a higher solubility in water of roughly 1 g/30 ml [5]. The CR dye is used in many industries, especially the textile industries, where wastewater containing this dye is discharged to industrial wastewater, and its quantities vary according to the industry type [6]. CR is a non-biodegradable and toxic dye that reaches the watercourse and accumulates in the bodies of living organisms, causing environmental and health problems for humans, such as cancer, kidney failure, oral ulceration, and anemia, as well as issues for animals and plants [7]. Therefore, industrial wastewater must be treated before being thrown into the watercourse to ensure health protection [8]. Many physical and chemical procedures, such as adsorption [9,10], reverse osmosis [11], coagulation [12], flocculation [13], membrane technology [14,15], and biological treatments used to adsorb dyes from aqueous solutions [16,17]. However, in developing nations, these methods remain prohibitively expensive. Adsorption is an efficient, fast, and economical electro-physical process widely used to remove many pollutants types [18]. Economical and available adsorbent materials are used, such as agricultural waste, such as rice husks [19], coconut husks [20], fly ash [21], and Cordia Myxa fruit [22], and agricultural waste [22,23]. Biochar is often developed during the thermochemical conversion of organic waste at 350–750 °C under limited oxygen conditions [24]. As an adsorbent, biochar functions best in a particular environment. Temperature, solution pH, concentrations, and Dye/biochar all affect how effective biochar is [25]. Many studies concern manufacturing and biochar use as an adsorbent to remove pollutants [26]. Nickel-modified biochar was capable of adsorbing the dye with a removal efficiency and adsorption capacity of 73% and 480 mg/g, respectively, from wastewater at 20 °C initially when the CR concentration was low, the removal efficiency by biochar was high (87%) due to a large number of active sites on the biochar for adsorption [27]. Similarly, Yek et al. [28] studied CR adsorption using peel waste. They found that the removal efficiency was 85 %. The results obtained in this study [28] were like that of [27]. Liu et al. conducted experiments for different concentrations of CR and FexCo3-xO4 dosages. The maximum qe of CR onto FexCo3-xO4 was 129 mg/g. The CR's adsorption declined, i.e., to 79.6% from 86% as the CR initial concentration rose from 10.1 mg/l to 30.1 mg/l. The authors found that a pseudo-first-order kinetic model fitted the results. The equilibrium adsorption data were also fitted using isotherm models, with the Langmuir and Freundlich equations shown appropriately [29]. Mahmoud et al. [30] prepared corncob nanobiochar (NCB) by carbonization; it was low-efficiency of the anionic dyes, but with high efficiency of the cationic dyes. They chosed Triethylenetetramine to bind with (NCB) to

result (NCB-TA). The NCB-TA was treated with sulfuric acid to produce positively charged amin nanobiochar (NCB-TA-PC) to improve the surface properties. Using Buckthorn fruit as biochar, Mohammadi et al. [31] conducted a study to remove lead from an aqueous solution. To characterize the equilibrium isotherms, the Langmuir and Freundlich equations were fitted to the data. As a result of activating biochar with H3PO4 and ZnCl2, the lead highest adsorption capacity on the resulting activated carbons was 51.8 mg/g and 25.9 mg g−1, respectively. The organic dye adsorption using agricultural biochar was conducted, and different functions' effects were examined [29]. pH effect was concerned [32], the authors noted that the dye removal efficiency declined by 5.1% when the pH was changed from 3 to 11. The removal efficiency decreased in a non-uniform manner between pH values of 3 and 9, but it declined sharply at pH 11 [19]. The present study investigates the possibility of using Buckthorn fruit as a low-cost adsorbent and eco-friendly to remove CR from aqueous solutions. Also, the present work studies the effect of pH, adsorbent dose, CR initial concentration, contact time, and mixing speed on the removal efficiency.

2.MATERIALS AND METHODS

2.1.Congo Red Dye (CR)

The Congo red dye (CR) (Chemical formula $C_{32}H_{22}N_6Na_2O_6S_2$, molecular weight of 696.6 g/mol, and maximum wavelength of 499 nm) [33, 34], supplied by the AGFA Company of Berlin and purchased from Alhekma market. CR is a good solvent in water, i.e., better in organic liquids such as alcohol. A red colloidal solution is formed as CR dissolves in water. In this study, CR was employed as an adsorbate. Distilled water was used to prepare the stock solution. 0.1 M HCl and 0.1 M NaOH were used for pH adjustment [35]. A pH meter (HANNA model HI2211; Indonesia) was used to measure the pH, a UV-VIS Spectrophotometer (Single Beam, Spectro UV-2550, Norway) was used to measure the CR concentrations, and a shaker water bath to perform the mixing process.

2.2.Activated Carbon from Buckthorn Fruit (BT) Preparation

Buckthorn fruit (BT) was used as an eco-friendly, low-cost, and locally available in the market adsorbent. Buckthorn Fruit is grown in Basra southern Iraq. Buckthorn Fruit was washed well with distilled water, then dried in the open air for 15 to 25 days until it was dried completely, crushed well, and sieved using a 100 mesh [36]. The powder was put into the furnace (Saftherm, China) at 700°C for 120 minutes, using Nitrogen at 100 mL/min flow rate [37]. The temperature in the tubular furnace was set to rise by 5°C every minute for 90 minutes, or until it reached 600°C. The product was removed from the furnace after the temperature was set at 600 °C for 120 minutes, and then progressively dropped for 1.5 hours to reach room temperature. To remove impurities, the resulted carbon was soaked in 0.5 M HCl for one day. The distilled water was used to wash the final product to obtain pH 7-liquid [21]. Using an electric oven at 105°C for 120 minutes to dry the product. The product was activated using HCl at 0.5 M to produce BT-A adsorbent.

2.3.Properties of the Produced Activated Carbon (BT-A)

The total pore volume (VT), i.e., P/Po = 0.99, and the BET surface area of BT-A utilizing a surface area analyzer (surface area analyzer, BELSORP, Microtrac Co. Japan) were determined using N2 adsorption-desorption isotherms [38]. Fourier-Transform Infrared Spectroscopy (FTIR) was used to examine the surface functional groups of BT-A. The Shimadzu 1800 FTIR spectrometer (Shimadzu, Japan) was utilized to examine the FTIR spectra of BT-A [38, 39]. The SEM (JSM-6060 LV, USA) observed the morphology of BT-A. With Cu Kα radiation (λ=1.54A°), the XRD device (Philips PW1730, Netherlands) was used for BT-A analyses. The scanning range for the samples was 5° to 80° (2θ).

2.4.Laboratory Experiments

A series of batch adsorption experiments were conducted using aqueous solutions prepared in the laboratory with different concentrations and conditions in terms of the initial concentration of the dye, pH of the solution, contact time, adsorbent dose, mixing speed, and temperature [40]. The experiments were conducted in a series of 100ml conical flasks using the Shaker water bath. Six samples of the CR solution were prepared with an initial concentration of 10 mg/l at a dose of the adsorbent of 0.3 g/100 ml. The pH value 3-9 was adjusted using 0.1 M HCl and 0.1 M NaOH, at a mixing speed of 150 rpm. The samples of the solutions are taken every 10 minutes until reaching equilibrium concentration which was measured using a UV-VIS Spectrophotometer after filtering the sample on 0.45µm filter paper [41]. The removal efficiency of CR was calculated from the following equation:

$$R\% = (C_O - C_e) \times 100 / C_O \quad \textbf{(1)}$$

where R = the efficiency of removal, C_o = initial concentration (mg/l), and C_e = effluent equilibrium concentration of CR (mg/l).

The adsorption capacity was calculated from the following equation:

$$q_e = (C_O - C_e) \times V/M \quad \textbf{(2)}$$

where q_e = adsorption capacity (mg/g), M =dosage(g), V)= volume of solution (l).

2.4.1.Adsorption Isotherm Models

The adsorption of various variables was linked to mathematical relations developed by several researchers called adsorption models [42]. To simulate and understand the adsorption, adsorption isotherms, i.e., mathematical equations, are used. The assumptions that these

equations depend on are the layers number the adsorbate accumulates on the adsorbents' surface, the adsorbent surface nature (homogeneous/heterogeneous), and the intermolecular reaction adsorbate possibility between it. These equations designate the distribution due to adsorbate pollutants between the liquid and solid phases [10]. The equations contain constants that describe the equilibrium process during isothermally adsorption, which reveals the surface adsorbents features and determines the affinity of the adsorbate with the adsorbent materials [43]. A curve can be drawn to describe the phenomenon that rules the retention (or mobility) or release of a substance from aqueous environments or aqueous porous medium to the solid phase at constant pH and temperature [44]. The adsorption model at equilibrium is important in determining the CR adsorption capacity. Most of the data obtained from the adsorption process can be represented by many models, including the Langmuir model, which is a theoretical relationship represented by the following equation:

$$C_e/q_e = (1/K_L \times q_{max}) + (C_e/q_{max}) \quad \textbf{(3)}$$

where q_e = adsorption capacity (mg/g), K_L = Langmuir's isotherm constant(l/mg), and q_{max} = maximum adsorption capacity(mg/g).

The other model was the Freundlich model, which was an experimental equation based on laboratory results which can be illustrated using the following equation:

$$q_e = k_f \times Ce^{1/n} \quad \textbf{(4)}$$

It can be formulated as a linear equation:

$$\log q_e = (1/n)\, \log Ce + \log k_f \quad \textbf{(5)}$$

where k_f = Freundlich adsorption capacity parameter (mg/g) $(l/mg)^{1/n}$, and 1/n = Freundlich adsorption intensity parameter, unitless.

2.4.2.Kinetic Models of Adsorption

The adsorption kinetics study is important in determining the efficiency of the adsorption process. Many kinetic models were used, including Pseudo-first-order, Pseudo-second-order, and Elovich kinetic models [9]. Pseudo-first-order kinetic model can be represented using the following equation:

$$\ln(q_e - q_t) = \ln q_e - K_1 t \quad \textbf{(6)}$$

where K_1= constant of kinetic equilibrium rate (min^{-1}), qt = the adsorbed mass per unit mass (mg/g) at any given time t, where t is the contact time (min). Pseudo-second-order can also be represented using the following equation:

$$t/qt = (1/K_2 \times qe^2) + (t/qe) \quad \textbf{(7)}$$

where K_2 (g/mg. min)= kinetic equilibrium rate constant. The Elovich relation can be represented using the following relation:

$$q_t = \beta \ln(\alpha\beta) + \beta \ln t \quad \textbf{(8)}$$

where α = initial adsorption rate (g/mg. min), and β = coefficient of desorption (mg/g.min), which equals the chemosorption activation energy.

2.4.3.Adsorption Thermodynamic

The changes in enthalpy (ΔH°), entropy (ΔS°), and Gibbs free energy (ΔG°) were calculated using the following equation:

$$K_d = qe/Ce \quad \textbf{(9)}$$

$$\ln(K_d) = (\Delta S/R) - (\Delta H/TR) \quad \textbf{(10)}$$

$$\Delta G° = \Delta H° - T\Delta S° \quad \textbf{(11)}$$

where Kd is the equilibrium thermodynamic constant (l/g), R is the universal gas constant (J/mol.K), i.e., 8.314 J/mol.K, T is solution temperature (K), and ΔH°, ΔS°, and ΔG° are the changes in enthalpy (J/mol), entropy (J/mol.K), and Gibbs free energy (J/mol), respectively.

3.RESULTS AND DISCUSSION

3.1. Prepared Activated Carbon (BT-A) Characterization

The N_2 adsorption and desorption isotherms results revealed that the adsorption/desorption isotherm was a type I according to the International Union of Pure and Applied Chemistry (IUPAC) classification, which means the presence of micropores [45] (Fig. 1). The method used to obtain the pore size distribution curve was Barrett-Joyner-Halenda (BJH). The pore diameter was 1.866 nm, the specific surface area was 774.1 m^2/g, and the total pore volume of BT-A was 0.361 cm^3/g. These results are near to [46] and [47]. The outcomes of the FTIR spectra on BT-A are shown in Fig. 2. With Quinone's carbonyl group C=O causing distinct peaks of the wavenumber at 1536.39 cm^{-1}, the sample may contain heavy metals or any other inorganic substance, as shown by the peaks smaller than 600 cm^{-1} [48]; The existence of the OH group, or moisture, in the sample, however, is explained by a wavenumber larger than 3000 cm^{-1}. This moisture may have entered the sample through the air during sample handling and analysis, as demonstrated by the wavenumber range from 3001.4 to 3627.92 cm^{-1} [49]. These outcomes align with the findings of [50-52]., the morphology of BT-A was scanned using SEM analysis (Fig. 3 (a), (b)). The view of the cross-sectional of BT-A is shown in Fig. 3 (a), (b) with x70-135 magnification, respectively. The porosity of BT-A is explained by SEM of BT-A after activation at the optimum conditions. It was found that the external surface contained less pores [43].

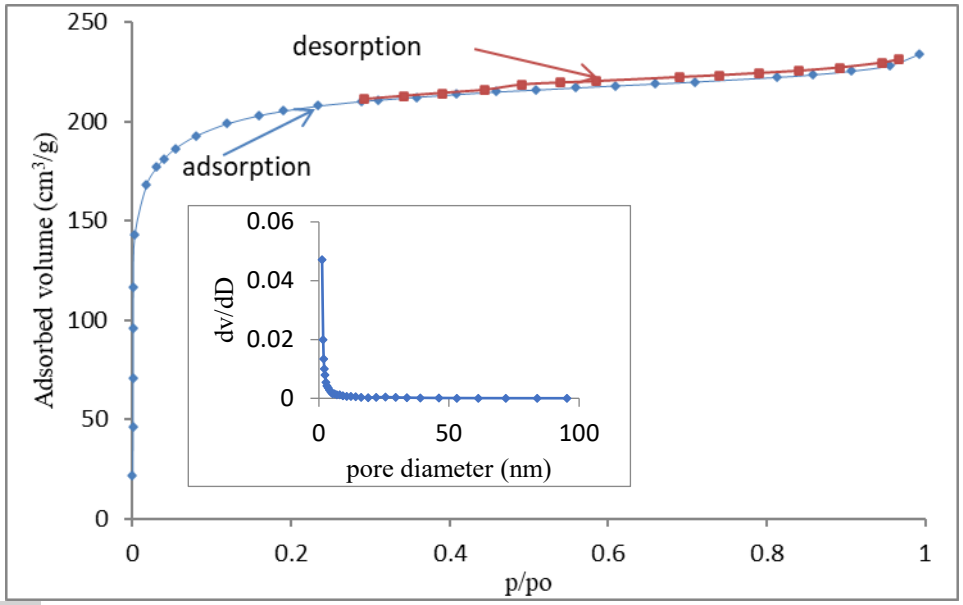

Fig. 1 N_2 Adsorption/Desorption Isotherm and Pore Size Distribution (Insert) of BT-A.

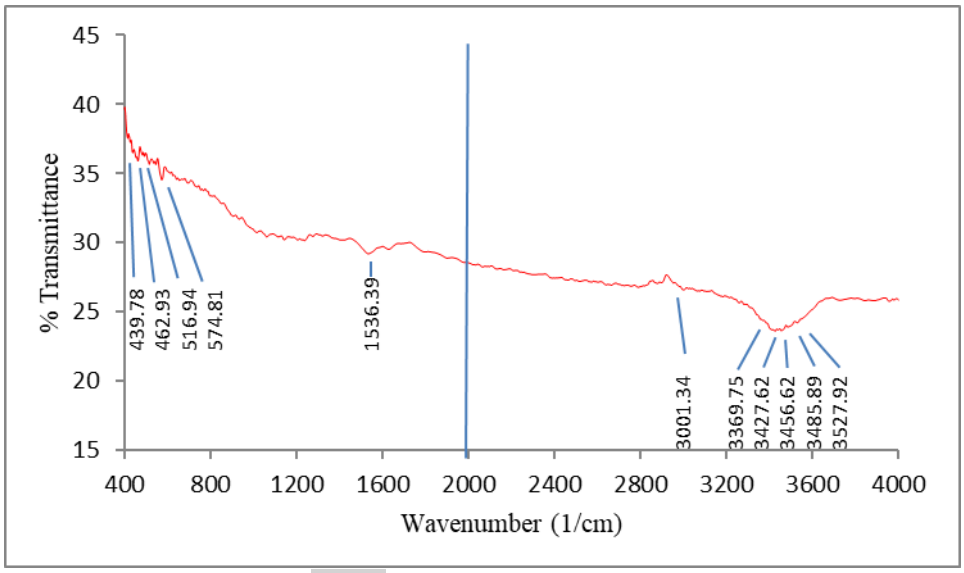

Fig. 2 FTIR Spectra of BT-A.

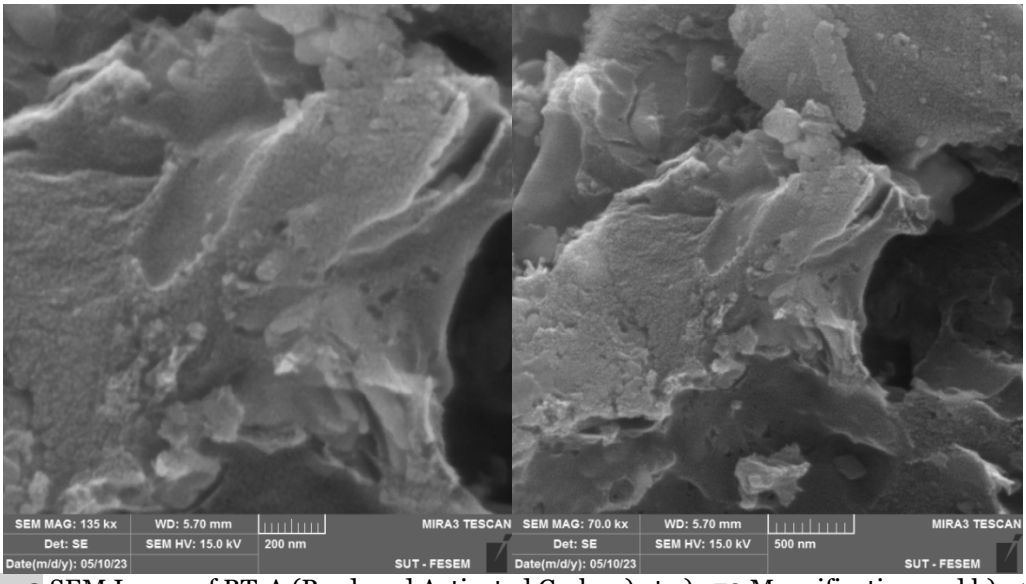

Fig. 3 SEM Image of BT-A (Produced Activated Carbon) at a) x70 Magnification and b) x135 Magnification.

The BT-A XRD patterns are shown in Fig. 4. The standard JCPDS file (41–1487) confirmed the crystalline structures formation of one of the carbon types, i.e., diffraction pattern well agrees at the peaks of (2θ) 26.386°, 29.958°, 42°, and 45° which corresponding to the peaks reflection (002), (121), (110), and (111) graphitic carbon crystal planes. It was clear that the prepared activated carbon's XRD pattern showed a sharp peak corresponding to reflection from the peak (002) plane at 26.386°, from the peak (121) plane at 29.958, from the peak (110) plane at 42°, and the peak (111) plane at 45° to d spacing of 0.337, 0.298, 0.215, and 0.201 nm, respectively, [44] and [45].

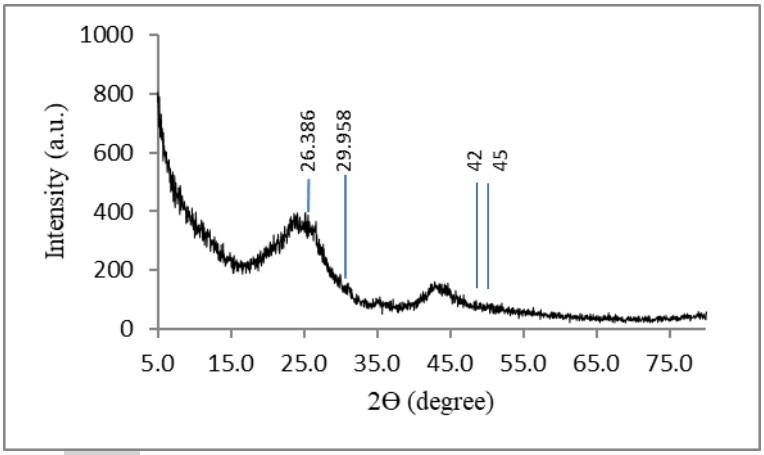

Fig. 4 XRD Analyses Obtained from BT-A Adsorbent.

3.2. pH Impact on CR Removal Efficiency

The effect of pH on the removal efficiency of CR onto BT-A is shown in Fig. 5. The contact time was measured from the adsorbent (BT-A) in addition to six samples of the aqueous solution prepared with equal concentrations of CR. pH was 3-9, and at room temperature. It was noted that the removal efficiency of CR increased with the contact time, and about 50% of adsorption was completed in the first 40 minutes until reaching equilibrium at 80 minutes in which the removal efficiency was almost constant. The maximum removal efficiency of CR dye, i.e., 63%, was at 80 minutes and pH=5, and an initial concentration of 10 mg/l. At pH= 5, both Congo Red and the BT-A adsorbent may have opposite charges. Congo Red is a negatively charged dye, while the BT-A adsorbent might carry a positive charge at pH= 5. This electrostatic attraction between the adsorbent and the dye can enhance the adsorption efficiency, resulting in a higher removal percentage. These results agrees with [17, 42].

3.3.Adsorbent (BT-A) Dose Effect on the Removal Efficiency of CR

The effect of the adsorbent dose on the removal efficiency of CR dye is shown in Fig. 6, where the efficiency of removal, Eq. (1), increased with the adsorption dose, i.e., from 0.5 to 10 g/l. The highest removal efficiency was 63% at adsorbent dosage of 3g/l, contact time of 80 min, mixing speed of 150 rpm, and pH = 5 due to the adsorbent surface area increase and exposure to a larger adsorption area [46]. An increase in the adsorbent dose decreased the adsorption capacity, Eq. (2). As the BT-A dose was increased by more than 3g/l, the CR removal efficiency slightly increased. As a result, from an economic point of view, the optimal dose was 3 g/l. These results are similar to [46–49].

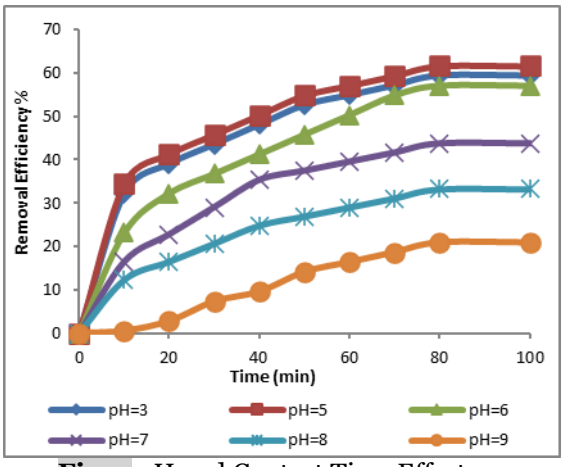

Fig. 5 pH and Contact Time Effect on Removal of CR onto BT-A (Temperature= 25°C, dose= 3g/l, and CR= 10mg/l).

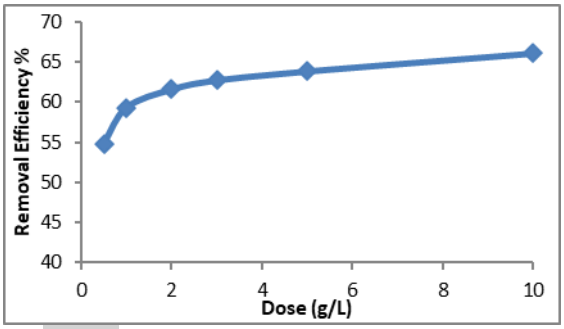

Fig. 6 The Dose of BT-A Effect of on the Efficiency of Removal of CR (Temperature= 25°C, pH=5, and CR= 10mg/l).

3.4.Adsorbate Concentration Effect on the CR Adsorption onto BT-A Adsorbent

Figure 7 shows the relationship between the removal efficiency and initial CR concentration . The removal efficiency decreased with rising the dye concentration, reaching the peak 63% at a 10 mg/l CR concentration. Then, the removal efficiency decreased with decreasing the dye's initial concentration due to competition for adsorption sites.

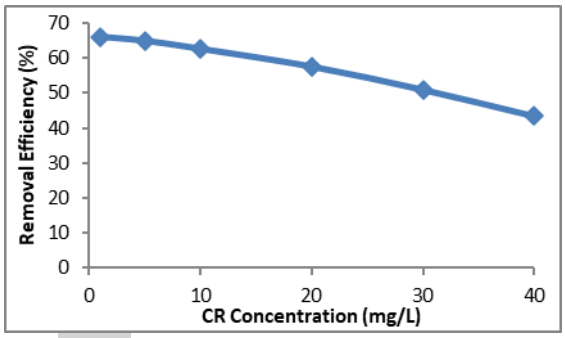

Fig. 7 CR Concentration Effect on the Efficiency of Removal by BT-A (Temperature= 25°C, dose= 3g/L, and pH=5).

3.5.Adsorption Isotherm Models

When drawing the relationship between $1/q_e$ and $1/c_e$, the K_L and q_{max} values can be calculated by applying Eq. 3 (Fig. 8).

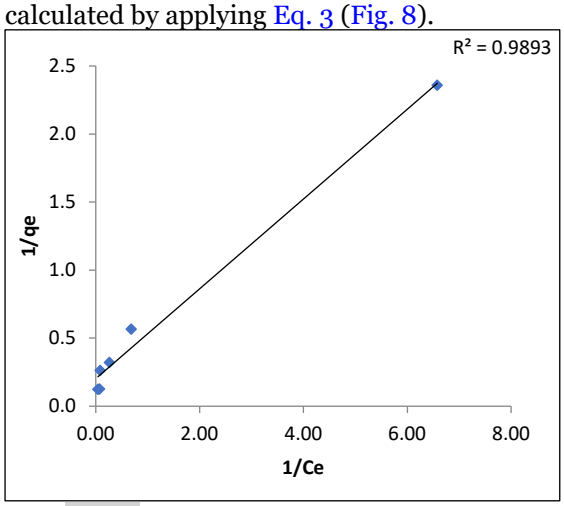

Fig. 8 Langmuir Isotherm Model for Adsorption of CR onto BT-A (Temperature= 25°C, Dose= 3g/l, and CR= 10mg/l).

However, when drawing the relationship between logce and logqe, the value of K_f can be calculated from the intersection of the straight line with the coordinates and the 1/n value from the slope of the straight-line Eq. (4) (Fig. 9). Table 1 shows the constants of the two models and shows that the data of the experiments can be represented using the Langmuir and Freundlich models. The Langmuir model was better than Freundlich, which means that the adsorption of CR dye on BT-A was the monolayer type, where the dye molecules adsorbed on a specific location on the surface of the BT-A adsorbent. Parallel results can be seen in the literature [47-48].

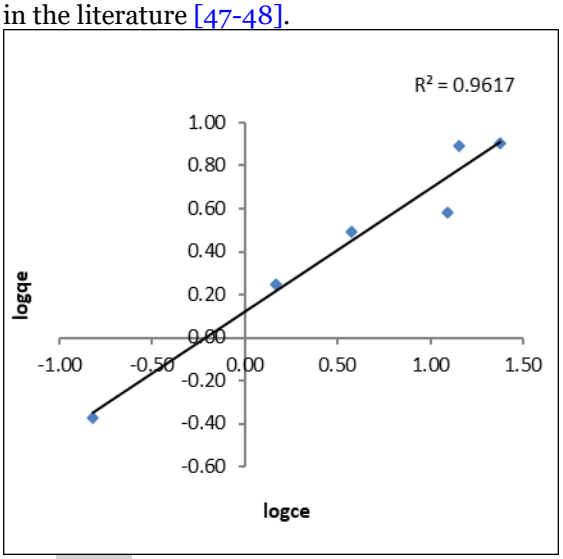

Fig. 9 Freundlich Isotherm Model for Adsorption of CR onto BT-A (Temperature= 25°C, Dose= 3g/l, and CR= 10mg/l).

Table 1 The Values and Units of the Adsorption Models Applied to the Adsorption of CR Dye onto BT-A.

Isotherm Model	Unit	Value
Langmuir	qmax (mg/g)	4.95
	KL(l/mg)	0.61
	R^2	0.989
Freundlich	1/n	0.572
	Kf (mg/g)(l/mg)1/n	1.127
	R^2	0.962

3.6.Kinetic Study Models

The pseudo-first-order, pseudo-second-order, and Elovich kinetic models (Eqs. (6-8)) were used to compute the adsorption rate and removing CR's regulating mechanism. If the trend line passed over as many of the points as feasible, the qe's model's projected value was adjacent to the experimental value, and the R^2 value was close to 1, i.e., the suitable model. The pseudo-second-order model best represented the practical data with K_2=0.083 g/mg.min and R^2=0.993 (Figs. 10 (a, b, c)) and (Table 2). These results are consistent with the findings of [32, 49].

Table 2 Adsorption Kinetic Models for Adsorption of CR onto BT-A.

Kinetic model	Parameter	Value
The pseudo-first-order	qe. calculated	5.317
	qe. experimental	15
	K_1	0.00006
	R^2	0.057
The pseudo-second-order	qe. calculated	14.16
	qe. experimental	15
	K_2	0.083
	R^2	0.993
Elovich	α	14.36
	β	0.476
	R^2	0.96

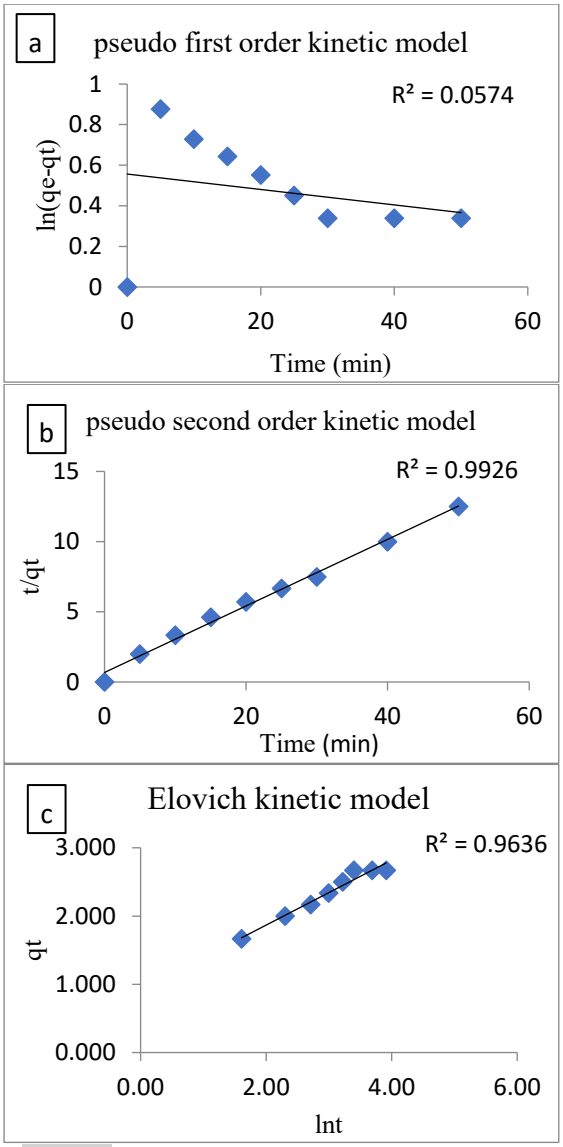

Fig. 10 (a) Pseudo-First-Order, (b) Pseudo-Second-Order, (c) Elovich Models to Examine the Adsorption Behavior of CR onto BT-A (25°C, dose= 3g/l, and CR= 10mg/l).

3.7.Adsorption Thermodynamics

The enthalpy (ΔH°), entropy (ΔS°), and Gibbs free energy (ΔG°) changes were calculated utilizing a sample of 100 mg/l of CR to indicate the thermodynamic parameters. The experiment conducted was under the modified circumstances of mixing speed of a 150-rpm, a temperature of 25°C, activated carbon as the adsorbent dose of 3 g/l, and a pH of 5. After estimating Ce using a UV-VIS spectrophotometer, the qe and K_d were calculated using Eq. (2) and Eq. (9), respectively. To find ΔH, ΔS, and ΔG at 25, 35, and 45°C and at the pH optimal values, adsorbent dose, and adsorbate concentration, the experiments as mentioned earlier were repeated under similar conditions, except changing the temperature to 35 and 45°C. From the relationship between 1/T and ln(K_d) plot, and according to Eq. (10), ΔH and ΔS were determined, and ΔG was calculated from Eq. (11) (Figs. (11, 12)). The adsorption interaction was endothermic, as indicated using the ΔH° of 13.709 kJ/mole. The ΔS° value was 48.3 J/mole.K, which indicated a particular structural modification and reduced system regularity in the solid/liquid interface. In contrast, the ΔG° values at 25°C, 35°C, and 45°C were negative, indicating a spontaneous adsorption interaction(Table 3). Similar results are found in numerous literatures [46, 49].

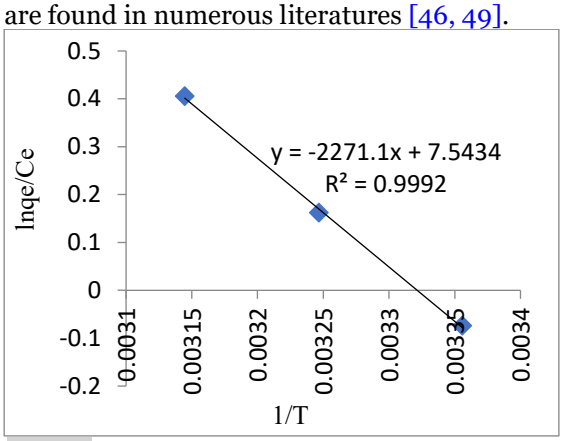

Fig. 11 Thermodynamic for the Adsorption (ln (qe/Ce) vs. 1/T (K)).

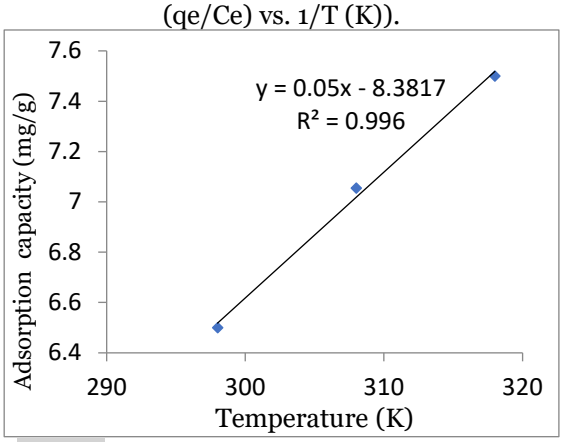

Fig. 12 Effect of Temperature on Adsorption Capacity (qe vs Temperature (K)).

Table 3 The Parameters of Thermodynamic for CR Removal onto BT-A.

Temperature (°C)	Temperature (K)	K_d (q_e/C_e)	ΔG° (kJ/mol)	ΔH° (kJ/mol)	ΔS° (J/mol.K)	R^2
25	298	1.33	-0.713			
35	308	1.58	-1.167	13.709	48.3	0.998
45	318	1.89	-1.681			

4.CONCLUSIONS

The present study showed the possibility of using Buckthorn fruit as a low-cost adsorbent to remove Congo red from solutions and industrial waste. The removal efficiency of Congo red dye depends on variables determined using batch pattern experiments, such as the solution pH and its optimal values (7-8). The best contact time to reach the adsorption equilibrium was 80 minutes.

Adsorption models were applied, and the best model representing the Congo red dye adsorption onto BT-A was the Langmuir model, so the value of R^2 = 0.989. The highest removal efficiency was 62% at a dose of 3 g/l, contact time of 80 minutes, a temperature of 25° C, and pH = 5. The adsorbent from Buckthorn fruit was low-cost and environmentally friendly because it was abundant and harmless.

REFERENCES

[1] Ahmed SH, Ibrahim AK, Abed MF. **Assessing the Quality of the Groundwater and the Nitrate Exposure, North Salah Al-Din Governorate, Iraq: Quality of Groundwater.** *Tikrit Journal of Engineering Sciences* 2023;**30**(1):25–36.

[2] Al-Taai SHH. **Soil Pollution-Causes and Effects**. *IOP Conference Series: Earth And Environmental Science* 2021; **790**(1): 12009, (1-14).

[3] He L, Michailidou F, Gahlon HL, Zeng W. **Hair Dye Ingredients and Potential Health Risks from Exposure to Hair Dyeing.** *Chemical Research in Toxicology* 2022;**35**(6):901–915.

[4] Chung K-T. **Azo Dyes and Human Health: A Review.** *Journal of Environmental Science and Health, Part C* 2016;**34**(4):233–261.

[5] Ali HQ, Mohammed AA. **Elimination of Congo Red Dyes from Aqueous Solution Using Eichhornia Crassipes**. *Iraqi Journal of Chemical and Petroleum Engineering* 2020;**21**(4): 21–32.

[6] Velusamy S, Roy A, Sundaram S, Kumar Mallick T. **A Review on Heavy Metal Ions and Containing Dyes Removal Through Graphene Oxide Based Adsorption Strategies for Textile Wastewater Treatment.** *The Chemical Record* 2021;**21**(7):1570–1610.

[7] Corda NC, Kini MS. **A Review on Adsorption of Cationic Dyes Using Activated Carbon**. *MATEC Web of Conferences* 2018; **144**:02022, (1-16).

[8] Ilyas M, Ahmad W, Khan H, Yousaf S, Yasir M, Khan A. **Environmental and Health Impacts of Industrial Wastewater Effluents in Pakistan: A Review.** *Reviews on Environmental Health* 2019;**34**(2):171–186.

[9] Al-Ghouti MA, Da'ana DA. **Guidelines for The Use and Interpretation of Adsorption Isotherm Models: A Review.** *Journal of Hazardous Materials* 2020;**393**:122383, (1-22).

[10] Joo SH, Tansel B. **Novel Technologies for Reverse Osmosis Concentrate Treatment: A Review.** *Journal of Environmental Management* 2015; **150**: 322–335.

[11] Ibrahim AK. **Effect of The Horizontal Perforated Plates on The Turbidity Removal Efficiency in Water Treatment Plant of Tikrit University.** *Tikrit Journal of Engineering Sciences* 2019;**26**(4):38–42.

[12] Ibrahim AK. **Improvement of Removal Efficiency of Water Supply Plant by Using Polyelectrolyte Type LT-22 with Alum**. *Materials Today: Proceedings* 2021;**42**:1928–1933.

[13] Politano A, Cupolillo A, Di Profio G, Arafat HA, Chiarello G, Curcio E. **When Plasmonics Meets Membrane Technology.** *Journal of Physics: Condensed Matter* 2016;**28**:363003.

[14] Li NN, Fane AG, Ho WSW, Matsuura T. **Advanced Membrane Technology and Applications**. Newjersey: John Wiley & Sons; 2011.

[15] Paz A, Carballo J, Pérez MJ, Domínguez JM. **Biological Treatment of Model Dyes and Textile Wastewaters**. *Chemosphere* 2017;**181**:168–177.

[16] Castro E, Avellaneda A, Marco P. **Combination of Advanced Oxidation Processes And Biological Treatment for The Removal of Benzidine Derived Dyes.** *Environmental Progress & Sustainable Energy* 2014;**33**(3):873–885.

[17] Adegoke KA, Olagunju AO, Alagbada TC, Alao OC, Adesina MO, Afolabi IC, Adegoke R O, & Bello O S. **Adsorptive Removal of Endocrine-Disrupting Chemicals from Aqueous Solutions: A Review.** *Water, Air, & Soil Pollution* 2022; **233**(2): 1–83.

[18] Tsai CY, Lin PY, Hsieh SL, Kirankumar R, Patel AK, Singhania RR,. **Engineered Mesoporous Biochar Derived from Rice Husk for Efficient Removal of Malachite Green from Wastewaters.** *Bioresource Technology* 2022; **347**: 126749, (1–8).

[19] Khaniabadi YO, Basiri H, Nourmoradi H, Mohammadi MJ, Yari AR, Sadeghi S, Amran A. **Adsorption of Congo Red Dye from Aqueous Solutions by Montmorillonite as a Low-Cost Adsorbent**. *International Journal of Chemical Reactor Engineering* 2018;**16**(1): 20160203.

[20] Mall ID, Srivastava VC, Agarwal NK, Mishra IM. **Removal of Congo Red from Aqueous Solution by Bagasse Fly Ash and Activated Carbon: Kinetic Study and Equilibrium Isotherm Analyses**. *Chemosphere* 2005;**61**(4):492–501.

[21] Amirza MAR, Adib MMR, Hamdan R. **Application of Agricultural Wastes Activated Carbon for Dye Removal -**

An Overview. *MATEC Web of Conferences* 2017;**103**: 06013, (32–42).

[22] Ezeonuegbu BA, Machido DA, Whong CMZ, Japhet WS, Alexiou A, Elazab ST, Qusty N, Yaro CA, Bateha G. **Agricultural Waste of Sugarcane Bagasse As Efficient Adsorbent for Lead and Nickel Removal from Untreated Wastewater: Biosorption , Equilibrium Isotherms, Kinetics and Desorption Studies**. *Biotechnology Reports* 2021;**30**:e00614, (1-10).

[23] Wu J, Yang J, Feng P, Huang G, Xu C, Lin B. **High-Efficiency Removal of Dyes from Wastewater by Fully Recycling Litchi Peel Biochar**. *Chemosphere* 2020;**246**:125734.

[24] Fan S, Tang J, Wang Y, Li H, Zhang H, Tang J, Wang Z, Li X. **Biochar Prepared from Co-Pyrolysis of Municipal Sewage Sludge and Tea Waste for The Adsorption of Methylene Blue from Aqueous Solutions: Kinetics, Isotherm, Thermodynamic and Mechanism.** *Journal of Molecular Liquids* 2016;**220**:432–441.

[25] Côrtes LN, Druzian SP, Streit AFM, Godinho M, Perondi D, Collazzo GC, Oliveira MLS. **Biochars from Animal Wastes as Alternative Materials to Treat Colored Effluents Containing Basic Red 9**. *Journal of Environmental Chemical Engineering* 2019;**7**(6):103446.

[26] Yek PNY, Peng W, Wong CC, Liew RK, Ho YL, Mahari WAW, Azwar E,Yuan TQ, Tabatabaei M, Aghbashlo M, Sonne C, Lam SS. **Engineered Biochar Via Microwave CO2 And Steam Pyrolysis to Treat Carcinogenic Congo Red Dye**. *Journal of Hazardous Materials* 2020;**395**:122636, (1-9).

[27] Mahmoud ME, Abdelfattah AM, Tharwat RM, Nabil GM. **Adsorption of Negatively Charged Food Tartrazine and Sunset Yellow Dyes onto Positively Charged Triethylenetetramine Biochar: Optimization, Kinetics and Thermodynamic Study.** *Journal of Molecular Liquids* 2020;**318**:114297.

[28] Goswami L, Kushwaha A, Kafle SR, Kim BS. **Surface Modification of Biochar for Dye Removal from Wastewater**. *Catalysts* 2022;**12**(8):817, (1-27).

[29] Liu J, Wang N, Zhang H, Baeyens J. **Adsorption of Congo Red Dye on FexCo3-xO4 Nanoparticles.** *Journal of Environmental Management* 2019; **238**: 473–483.

[30] Mohammadi SZ, Karimi MA, Afzali D, Mansouri F. **Removal of Pb (II) from Aqueous Solutions Using Activated Carbon from Sea-Buckthorn Stones by Chemical Activation**. *Desalination* 2010;**262**(1-3):86–93.

[31] De Leo V, Maurelli AM, Ingrosso C, Lupone F, Catucci L. **Easy Preparation of Liposome@PDA Microspheres for Fast and Highly Efficient Removal of Methylene Blue from Water.** *International Journal of Molecular Sciences* 2021;**22**(21): 11916, (1-17).

[32] Ravi R, Iqbal S, Ghosal A, Ahmad S. **Novel Mesoporous Trimetallic Strontium Magnesium Ferrite (Sro. 3Mgo. 7Fe2O4) Nanocubes: a Selective and Recoverable Magnetic Nanoadsorbent for Congo Red.** *Journal of Alloys and Compounds* 2019;**791**:336–347.

[33] Litefti K, Freire MS, Stitou M, González-Álvarez J. **Adsorption of an Anionic Dye (Congo Red) from Aqueous Solutions by Pine Bark**. *Scientific Reports* 2019;**9**(1):16530, (1–11).

[34] Dawood S, Sen TK, Phan C. **Synthesis and Characterisation of Novel-Activated Carbon from Waste Biomass Pine Cone and its Application in the Removal of Congo Red Dye from Aqueous Solution by Adsorption**. *Water, Air, & Soil Pollution* 2014;**225**:1–16.

[35] Morin M, Pécate S, Masi E, Hémati M. **Kinetic Study and Modelling Of Char Combustion in TGA In Isothermal Conditions**. *Fuel* 2017;**203**:522–536.

[36] Bayati M, Numaan M, Kadhem A, Salahshoor Z, Qasim S, Deng H, Len J, Yan Z, Lin C, Cortalezzi M. **Adsorption of Atrazine by Laser Induced Graphitic Material: an Efficient, Scalable and Green Alternative For Pollution Abatement.** *Journal of Environmental Chemical Engineering* 2020;**8**(5): 104407.

[37] Jung MR, Horgen FD, Orski S V, Rodriguez V, Beers KL, Balazs GH, Todd T. **Validation of ATR FT-IR to Identify Polymers of Plastic Marine Debris, Including Those Ingested by Marine Organisms**. *Marine Pollution Bulletin* 2018;**127**:704–716.

[38] Feng Fu, Gao Z, Gao L, Li D. **Effective Adsorption of Anionic Dye, Alizarin Red S, from Aqueous Solutions on Activated Clay Modified by Iron Oxide.** *Industrial & Engineering Chemistry Research* 2011;**50**:9712–9717.

[39] Shi Q-X, Li Y, Wang L, Wang J, Cao Y-L. **Preparation of Supported Chitosan Adsorbent with High Adsorption Capacity for Titan Yellow Removal.** *International Journal of Biological*

Macromolecules 2020;**152**:449–455.

[40] Gerente C, Lee VKC, Cloirec P Le, McKay G. **Application of Chitosan for the Removal of Metals from Wastewaters by Adsorption—Mechanisms and Models Review.** *Critical Reviews in Environmental Science and Technology* 2007;**37**(1):41–127.

[41] Milmile SN, Pande JV, Karmakar S, Bansiwal A, Chakrabarti T, Biniwale RB. **Equilibrium Isotherm and Kinetic Modeling of the Adsorption of Nitrates by Anion Exchange Indion NSSR Resin**. *Desalination* 2011; **276**(1-3):38–44.

[42] Ligotski R, Sager U, Schneiderwind U, Asbach C, Schmidt F. **Prediction of VOC Adsorption Performance for Estimation of Service Life of Activated Carbon Based Filter Media for Indoor Air Purification.** *Building and Environment* 2019; **149**: 146–156.

[43] Elmouwahidi A, Bailón-García E, Castelo-Quibén J, Pérez-Cadenas AF, Maldonado-Hódar FJ, Carrasco-Marín F. **Carbon–TiO 2 Composites as High-Performance Supercapacitor Electrodes: Synergistic Effect Between Carbon and Metal Oxide Phases.** *Journal of Materials Chemistry A* 2018;**6**(2):633–644.

[44] Torres-Pérez J, Gérente C, Andrès Y. **Sustainable Activated Carbons from Agricultural Residues Dedicated to Antibiotic Removal by Adsorption.** *Chinese Journal of Chemical Engineering* 2012;**20**(3):524–529.

[45] Khurshid H, Mustafa MRU, Rashid U, Isa MH, Ho YC, Shah MM. **Adsorptive Removal of COD from Produced Water Using Tea Waste Biochar**. *Environmental Technology & Innovation* 2021;**23**:101563.

[46] Tang H, Liu F, Wei J, Qiao B, Zhao K, Su Y, Jin C, Li L, Liu J, Wang J, Zhang T. **Ultrastable Hydroxyapatite/ Titanium Dioxide Supported Gold Nanocatalyst with Strong Metal–Support Interaction for Carbon Monoxide Oxidation**. *Angewandte Chemie International Edition* 2016;**55**(36):10606–10611.

[47] Zhang X, Bai B, Puma GL, Wang H, Suo Y. **Novel Sea Buckthorn Biocarbon SBC@ B-Feooh Composites: Efficient Removal of Doxycycline in Aqueous Solution in a Fixed-Bed Through Synergistic Adsorption and Heterogeneous Fenton - Like Reaction.** *Chemical Engineering Journal* 2016;**284**:698–707.

[48] Ahmed SH. **Cu II Removal from Industrial Wastewater Using Low Cost Adsorbent**. *Tikrit Journal of Engineering Sciences* 2017;**24**(2): 40-50.

[49] Ibrahim AK, Ahmed SH, Abduljabbar RA. **Removal of Methylene Blue Dye from Aqueous Solutions Using Cordia Myxa Fruits as a Low-Cost Adsorbent**. *Tikrit Journal of Engineering Sciences* 2023;**30**(3):90–99.